Chemical Physics Letters 507 (2011) 48–51

Contents lists available at ScienceDirect

Chemical Physics Letters

journal homepage: www.elsevier.com/locate/cplett

First-principles rotation–vibration spectrum of water above dissociation

Nikolay F. Zobov [a], Sergei V. Shirin [a], Lorenzo Lodi [b], Bruno C. Silva [b], Jonathan Tennyson [b,*], Attila G. Császár [c], Oleg L. Polyansky [a,b]

[a] Institute of Applied Physics, Russian Academy of Sciences, Uljanov Street 46, Nizhnii Novgorod 603950, Russia
[b] Department of Physics and Astronomy, University College London, London WC1E 6BT, UK
[c] Institute of Chemistry, Laboratory of Molecular Spectroscopy, Loránd Eötvös University, P.O. Box 32, H-1518 Budapest 112, Hungary

ARTICLE INFO

Article history:
Received 7 January 2011
In final form 17 March 2011
Available online 21 March 2011

ABSTRACT

High-level *ab initio* electronic structure and variational nuclear motion computations are combined to simulate the spectrum of the water molecule at and above its first dissociation limit. Results of these computations are compared with the related state-selective multi-photon measurements of Grechko et al. [J. Chem. Phys. 138 (2010) 081 103]. Both measured and computed spectra show pronounced structures due to quasi-bound (resonance) states. Traditional resonance features associated with trapping of vibrational or rotational energy of the system are identified and assigned. A strong and broad feature observed slightly above dissociation is found to be associated with direct photodissociation into the continuum.

1. Introduction

Much of chemistry involves the joining together and breaking up of molecules to form new species. Therefore, understanding just how molecules behave around the point of dissociation is fundamental for studies of chemical reactions. The photodissociation of the water molecule is a thoroughly investigated [1–3], even textbook-type [4] problem in chemical physics. However, in its traditional interpretation this process occurs exclusively via an electronically allowed transition to an excited electronic state. In this Letter we explore photodissociation on the ground-state surface by probing the structure of rotation–vibration states which lie at the first dissociation limit of water.

Detection of photodissociation on a ground-state surface is an extremely complex task both from an experimental and a theoretical point of view. Even the simplest polyatomic molecules have a large number of bound rotation–vibration states with energies below the first dissociation limit. A portion of the clusters of these states continue above dissociation where they have short lifetime and become quasibound or resonance states. These states determine fragmentation dynamics near dissociation and at the same time control low-temperature association reactions.

Previous studies of near-threshold resonance structures have largely defied analysis [5,6]. It is anticipated that two mechanisms lead to the formation of long-lived resonances. Rotational excitation leads to a centrifugal barrier behind which states can be trapped, giving origin to so-called shape resonances. Shape resonances, whose widths are determined by the centrifugal barrier, cause, for example, the multitude of unassigned lines observed in the near-dissociation spectrum of H_3^+ [5]. Vibrational excitation into non-dissociating states gives Feshbach (sometimes called Fano–Feshbach) resonances. Such resonances have been observed previously in molecular systems [7–11] and were also identified in a recent above-dissociation study of the water spectrum [12]. A combination of these two mechanisms is also possible [13].

In this study we report a first-principles quantum chemical investigation of the rotation–vibration states of water vapor beyond its first dissociation limit. Part of this study models the state-selective, triple-resonance spectra of Grechko et al. [12], which probed, for the first time, the structure of the near-threshold, photodissociation spectrum of water. These high-resolution spectra are simplified enormously by spectral selectivity originating from the rigorous selection rules governing the change of rotational angular momentum quantum number J ($\Delta J = 0,\pm1$), conservation of ortho–para symmetry and rotational parity for each transition. Further selection rules arise from the choice of the polarization of the laser in the experiments. The triple-resonance experiments result in well-resolved resonance lines, narrow enough to resemble the spectrum below dissociation [12], plus some broader structures. We demonstrate that the observed highly-structured spectra are due to several mechanisms: resonances stabilized by either vibrational (bending) or rotational excitation and, unusually, direct photodissociation into a structured continuum.

* Corresponding author.
E-mail address: j.tennyson@ucl.ac.uk (J. Tennyson).

0009-2614/$ - see front matter © 2011 Elsevier B.V. All rights reserved.
doi:10.1016/j.cplett.2011.03.052

2. Computational details

Understanding the observed spectra requires carrying out sophisticated electronic structure and nuclear motion computations. The use of an entirely *ab initio* procedure to model the spectrum is necessary because of the lack of information on the states in this region. This strategy places great demands on the accuracy of the spectroscopic computations to be performed in the near-dissociation region. The clamped-nuclei electronic energy values used to determine the potential energy surface (PES) were obtained from large basis set (aug-cc-pCV6Z) [14], all-electron, internally contracted multi-reference configuration interaction (MR-CI) [15] computations in an (8-electron, 10-orbital) active space augmented by first-order relativistic corrections and fitted to a flexible functional form appropriate for a dissociating system [16,17]. The resulting surface, which has been given as part of a study of vibrational levels up to dissociation [16,18], gives $D_0 = 41\,108\ \mathrm{cm}^{-1}$, only $38\ \mathrm{cm}^{-1}$ lower than the measured value of the first dissociation limit, $41\,145.94 \pm 0.15\ \mathrm{cm}^{-1}$ [19].

Variational nuclear motion procedures capable of giving the rotation–vibration levels of water up to dissociation are well established [20–25]. Above D_0, the initial step is the same as below D_0 [16] but an extended radial basis needs to be used. These computations were performed in Radau coordinates using the DVR3D program suite [26] for $J = 0$, 1, 2 and 3 (not all results are shown here) using 120 radial discrete variable representation (DVR) grid points and 38 angular DVR points; the final Hamiltonian matrix has dimension 15,000. Wave functions from these computations then formed the input for an automated resonance finding procedure [27], using a complex absorbing potential (CAP) [28] in the dissociative OH coordinates. Simple cubic polynomial CAPs were used over a variable range: r_{OH} from 8, 9 or 10 a_0 to 14.52 a_0, the latter being the final DVR grid point for a radial DVR of 120 points. Integrals over this CAP are straightforward to compute in a DVR. The automated procedure [27] uses as a basis the results of a CAP-free problem taking only functions lying directly above dissociation and, here, below $47\,000\ \mathrm{cm}^{-1}$. These functions are used to diagonalize the complex CAP Hamiltonian as function of CAP strength and the automated graphical search yields resonance positions, lifetimes, and associated wave functions localized in the resonance region. Tests with a larger DVR grid of 150 radial points suggested that the calculated resonance positions were stable to within $1\ \mathrm{cm}^{-1}$ and the resonance widths to within about a factor of two. Assignments were made using the four methods developed in [16] to characterize the spectrum up to dissociation: using expectation values to give quantum numbers, dependence of the energy levels on quantum numbers, visual inspection of wavefunction plots and the behavior of the energy levels upon artificial changes in the bending potential. These measures give us a fair degree of confidence in our rovibrational labels.

Transition intensities from the gateway state are computed using the CVR dipole moment surface [29], modified slightly to give correct asymptotic behavior. The intensities computed for the resonance features are rather sensitive to the CAP parameters employed and are in all probability not particularly accurate.

3. Results and discussion

Following Grechko et al. [6], we label our states $J_{KaKc}\ (m,n)^{\pm}\upsilon_2$, where the asymmetric top rotational quantum numbers J_{KaKc} are standard, the stretching vibrational quantum numbers $(m,n)^{\pm}$ use the local-mode notation [30], and υ_2 is the usual bending quantum number. Figure 1 gives a sample of the above-dissociation spectrum corresponding to the gateway state $1_{01}\ (90)^{+}0$ and shows that it becomes richly structured with both sharp and broad features.

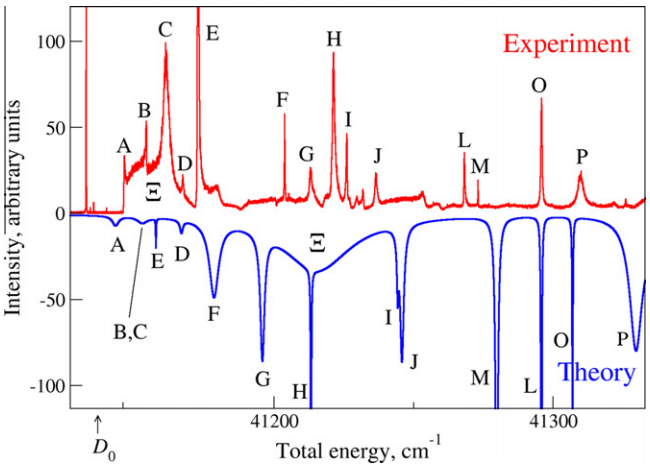

Figure 1. A state-selective, triple-resonance spectrum of water above dissociation, showing transitions from the gateway state [27561.25 cm^{-1};101$(90)^{+}$0] to states with $J = 0$ and 2. 'Experiment' corresponds to Figure 2b of Grechko et al. [12] and 'Theory' is as computed in this study and shifted by $38\ \mathrm{cm}^{-1}$. Features A–D are shape resonances, other Roman letters correspond to Feshbach resonances. Assignments for most of these features are given in Table 1. The broad and intense feature Ξ is discussed in detail in the text.

The theoretical frequency scale was shifted by $38\ \mathrm{cm}^{-1}$ to allow for the difference in the computed and measured D_0 values. This simple shift has the effect of moving most experimental and *ab initio* spectral features depicted on Figure 1 into approximate alignment. Unfortunately, the shift misaligns the broad feature Ξ. This appears to be a consequence of different sensitivity of the above-dissociation features to imperfections in the PES. Nevertheless, the considerable separation of the experimental features allows their unambiguous labeling based on the computed results. Since further substantial improvement of the PES in the dissociating region is rather problematic [18] except possibly for the inclusion of the spin–orbit effect, it seems that for resonances in many-electron polyatomic systems one has to live with uncertainties larger than what is usually achievable for bound states.

A direct comparison between our calculations and the experiment is complicated by two factors. First, the measurements were made using action spectroscopy which only monitored one of two possible exit channels [12] whereas we calculated total absorption. It is expected that the action spectra will preserve the approximate magnitudes of the absorption but with some variations in detail. Second, the measured spectrum displays a number of Fano line profiles with dips as well as peaks. Such profiles result from the interference between two different dissociation processes such a resonance superimposed upon a background arising from a direct dissociation continuum. Theoretically the full profile can only be obtained from treatment including a comprehensive treatment of the continuum states that would arise, for example, from a scattering calculation.

Our results on water suggest that in the above-dissociation region the two traditional types of absorption features can be characterized by theory using the CAP technique, at least when the spectra are simplified experimentally by state-selective excitation. Most narrow lines observed correspond to *Feshbach resonances*, in which the extra energy is stored in non-dissociating (bending) vibrational modes. These are the features denoted **E**–**P** in Figure 1. *Shape resonances* are also observed; these are due to levels whose $J = 0$ vibrational state is below dissociation but then rotational excitation brings the lines above the dissociation limit. These are the features **A**–**D** in Figure 1. Some of the minor experimental features remain unassigned; these are likely to be Feshbach

resonances with significant energy in the bending vibration. Our calculations are not fully reliable for such states due both to the relatively small angular basis employed and the quality of the PES.

Table 1 gives a comparison between the experimentally-measured energy levels and our calculated ones, including features observed using laser setups to the one to generate Figure 1. We note that our vibrational labels do not always agree with those of Grechko et al. [12]. We believe ours are the most probable labels for a number of reasons. Our assignments all correspond to states with $(m,0)^{\pm}v_2$ in local modes, with $v_2 = 0$, 1 or 2. This is to be expected as these are the extreme motion states, the ones which retain their character in the 'chaotic' regime, and the same pattern is observed below dissociation [16]. These states should dominate above dissociation as they retain their character and hence support resonances whereas 'chaotic' states will couple strongly to the continuum and hence have no significant lifetimes [9,31]. Furthermore, our calculations show that transitions to these extreme motion states have much the strongest dipole transitions. In practice, we can only be truly confident in assignments to local-mode states $(m,n)^{\pm}v_2$ with $n = 0$ and 1 combined with low values of v_2, since these labels could be confirmed by visual inspection of plots of the radial wave functions (see Figure 2 for an example). Issues with labeling high-lying vibrational states below dissociation have been discussed by us before [16].

There is one particularly strong feature in the experimental spectrum given in Figure 1 whose structure was not characterized as a resonance by our CAP computations. This third type of absorption feature is the ($\sim$40 cm^{-1}) wide structure, 'Ξ', just above dissociation. We believe this feature to be due to direct photodissociation via a continuum state which is strongly scarred by a phantom odd-parity $(20,0)^{-}0$ vibrational ($J = 0$) state, depicted in Figure 2. The computed transition intensity of this feature is significantly stronger than all others considered. We note that the $\sim$20 cm^{-1} half-width implies a lifetime of 0.25 ps, which corresponds to half a vibrational period for this mode.

Both members of the $J = 0$ $(20,0)^{\pm}0$ local mode pair, depicted in Figure 2, are involved in transitions with different characteristics. Unlike the odd feature, our calculations predicted the even, $(20,0)^{+}0$ feature as a 2 cm^{-1} wide resonance, in agreement with Grechko et al.'s observations (private communication). It seems that while the odd motion leads directly to dissociation, the even motion is initially trapped as a Feshbach resonance, albeit for only about 2 ps, before dissociating.

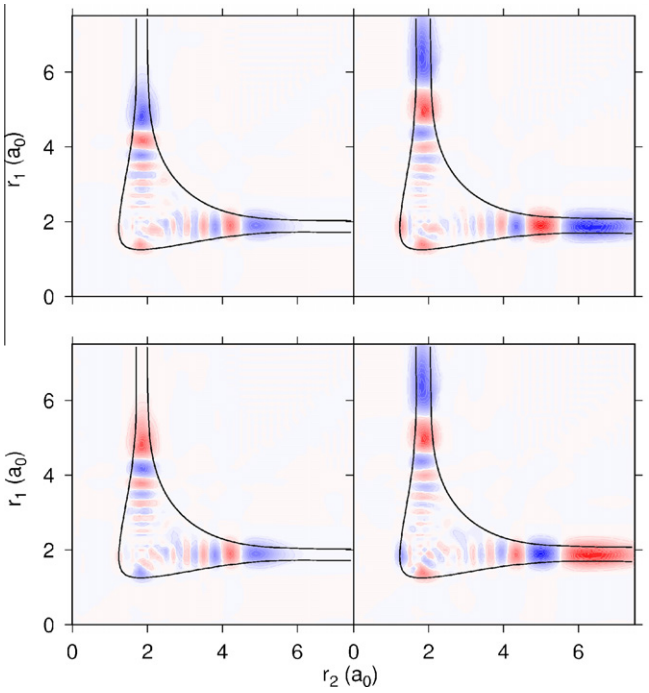

Figure 2. Plots of radial wave functions. Top row: $J = 0$ even states calculated to lie at 40405.2 cm^{-1} (left), assigned to $(17,0)^{+}0$ (Ref. [16]), and in the continuum (right) which is structured as $(20,0)^{+}0$. Bottom row: $J = 0$ odd states calculated to lie at 40405.4 cm^{-1} (left), assigned to $(17,0)^{-}0$ (Ref. [16]), and in the continuum (right) which is structured as $(20,0)^{-}0$. Coordinates r_1 and r_2 are Radau coordinates which, for water, are very close to the usual bond length coordinates. The plots are cuts for a bond angle of 110°; none of the states have significant nodal structure in the angular coordinate. The $(20,0)^{-}0$ state produces the broad structure labeled Ξ in Figure 1.

Table 1
Observed rotational–vibrational energy levels ('Energy') and widths (Γ), in cm^{-1}, of states assigned above the first dissociation limit of water. The experimental data and the line labels are taken from Table I of Grechko et al. [6]. The calculated broad feature was labeled as Ξ; the experimental parameters for this are our own estimates. The vibrational states are denoted by the local-mode labels $(m,n)^{\pm}v_2$,while the rotational–vibrational states are labeled by the usual asymmetric-top rigid-rotor labels $J\,K_a\,K_c$.

Grechko et al. [6]					This work		
Label	Energy	Γ	J	$(m,n)\pm v_2$	$J\,K_a\,K_c$ $(m,n)^{\pm}v_2$	Energy	Γ
Ξ	41160	15			$J = 0$	41177	20
A	41146.17	0.43	2	$(19,0)^{\pm}0$	2 0 2 $(19,0)^{-}0$	41105.2	1.30
B	41154.11	0.35	2	–	2 1 2 $(19,0)^{+}0$	41117.9	1.10
C	41161.24	2.4	2	$(18,0)^{\pm}1$	2 0 2 $(16,0)^{-}2$	41114.8	2.01
D	41167.24	0.60	2	$(12,2)^{\pm}0$	2 1 2 $(16,0)^{+}2$	41128.8	0.63
E	41172.67	0.21	0	$(13,1)^{-}2$	0 0 0 $(18,0)^{-}1$	41119.7	0.01
F	41203.73	0.22	0	–	$J = 0$	41140.5	2.03
G	41212.95	1.03	2	–	2 0 2 $(18,0)^{-}1$	41157.8	0.89
H	41221.23	1.00	0	$(9,4)^{-}0$	$J = 0$	41175.3	0.002
I	41225.99	0.42	0	–	$J = 0$	41206.3	0.33
J	41236.45	0.89	2	–	2 1 2 $(18,0)^{+}1$	41207.9	0.78
K	41263.56	0.09	0	$(8,4)^{-}2$	$J = 0$	41224.4	0.30
L	41268.09	0.36	0	$(19,0)^{-}1$	0 0 0 $(17,0)^{-}2$	41257.8	0.03
M	41273.03	0.10	2	–	$J = 2$	41241.8	0.10
N	41291.93	0.16	1	–	1 1 0 $(17,0)^{+}2$	41277.9	0.34
O	41295.77	0.52	0	$(18,0)^{-}2$	$J = 0$	41269.0	0.12
P	41309.76	2.4	0	–	$J = 0$	41275.1	20.14
Q	41314.90	1.3	2	$(8,4)^{-}2$	2 0 2 $(17,0)^{-}2$	41291.7	2.73
R	41317.18	0.38	2	$(8,4)^{+}2$	2 1 2 $(17,0)^{+}2$	41299.1	2.16

4. Conclusions

State-selective spectroscopy provides much simplified spectra and thus a detailed experimental probe of the rovibrational energy-level structure of water below and also above dissociation. We demonstrate here that above dissociation the complex resonance structures detected can be interpreted with the aid of sophisticated first-principles computations. We find that several mechanisms are responsible for the very pronounced structures observed experimentally [12] in the near-dissociation continuum of the water molecule. They include the traditional Feshbach and shape resonances, several of which were identified as part of this study. More unusually, a spectral feature corresponding to direct photodissociation to the continuum was also found.

The high precision, global, molecular potential energy surfaces resulting from the interplay of the availability of experimental state-selective spectra and spectral results from variational first-principles computations provide the tools for understanding chemical reactions occurring at low temperatures, which are expected to be sensitive to resonance structures and other quantum phenomena. Combined quantum mechanical and experimental studies of this nature could provide the only way forward to complete our understanding of the quantum behavior of molecules in dissociative regions. Note that the present work lays the basis for future improvement of the potential energy surface of water by either further *ab initio* studies or by fitting to the observed resonances. As our calculations reproduce the position of the gateway states to within 3 cm^{-1} [16], the major area for improvement is in the dissociative region. The aim would be not only to correct for the discrepancy with respect to the measured dissociation energy but also to allow for spin–orbit splitting present in the dissociated $^2\Pi_{3/2}$ OH fragment quenched in the ground-state water molecule.

Acknowledgements

We thank the experimental team of Maxim Grechko, Pavlo Maksyutenko, Thomas R. Rizzo, and Oleg V. Boyarkin for supplying their data prior to publication and for many very helpful discussions. We also thank Pavlo Maksyutenko for help with the initial electronic structure computations. This work was supported by the Russian Fund for Basic Research, EPSRC, NERC, the Royal Society, OTKA, ERA-Chemistry, the European Union, and the European Social Fund.

References

[1] R.L. Vander Wal, J.L. Scott, F.F. Crim, J. Chem. Phys. 94 (1991) 1859.
[2] P. Andresen, V. Beushausen, D. Häusler, H.W. Lülf, E.W. Rothe, J. Chem. Phys. 83 (1985) 1429.
[3] D. Häusler, P. Andresen, R. Schinke, J. Chem. Phys. 87 (1987) 3949.
[4] R. Schinke, Photodissociation Dynamics: Spectroscopy and Fragmentation of Small Polyatomic Molecules, Cambridge University Press, 1995.
[5] A. Carrington, I.R. McNab, Y.D. West, Chem. Phys. 98 (1993) 1073.
[6] J. Miyawaki, K. Yamanouchi, S. Tsuchiya, Chem. Phys. 99 (1993) 254.
[7] A. Callegari, R. Schmied, P. Theule, J. Rebstein, T.R. Rizzo, Chem. Chem. Phys. 3 (2001) 2245.
[8] X. Luo, T.R. Rizzo, Chem. Phys. 93 (1990) 8620.
[9] P.D. Chowdary, M. Gruebele, J. Chem. Phys. 130 (2009) 024305.
[10] S.A. Reid, H. Reisler, Annu. Rev. Phys. Chem. 47 (1996) 495.
[11] Y.S. Choi, C.B. Moore, J. Chem. Phys. 94 (1991) 5414.
[12] M. Grechko, P. Maksyutenko, T.R. Rizzo, O.V. Boyarkin, J. Chem. Phys. 133 (2010) 081103.
[13] H.Y. Mussa, J. Tennyson, Chem. Phys. Lett. 366 (2002) 449.
[14] T.H. Dunning Jr., J. Chem. Phys. 90 (1989) 1007.
[15] H.-J. Werner, P.J. Knowles, J. Chem. Phys. 89 (1988) 5803.
[16] A.G. Császár et al., J. Quant. Spectrosc. Rad. Transf. 111 (2010) 1043.
[17] L. Lodi, O.L. Polyansky, J. Tennyson, Mol. Phys. 106 (2008) 1267.
[18] M. Grechko et al., J. Chem. Phys. 131 (2009) 221105.
[19] P. Maksyutenko, T.R. Rizzo, O.V. Boyarkin, J. Chem. Phys. 125 (2006) 181101.
[20] P. Maksyutenko, J.S. Muenter, N.F. Zobov, S.V. Shirin, O.L. Polyansky, T.R. Rizzo, O.V. Boyarkin, J. Chem. Phys. 126 (2007) 241101.
[21] M. Grechko, P. Maksyutenko, N.F. Zobov, S.V. Shirin, O.L. Polyansky, T.R. Rizzo, O.V. Boyarkin, J. Phys. Chem. 112 (2008) 10539.
[22] H.Y. Mussa, J. Tennyson, J. Chem. Phys. 109 (1998) 10885.
[23] S.K. Gray, E.M. Goldfield, J. Phys. Chem. 105 (2001) 2634.
[24] G.H. Li, H. Guo, J. Molec. Spectrosc. 210 (2001) 90.
[25] L. Lodi, J. Tennyson, J. Phys. B: At. Mol. Opt. Phys. 43 (2010) 133001.
[26] J. Tennyson, M.A. Kostin, P. Barletta, G.J. Harris, O.L. Polyansky, J. Ramanlal, N.F. Zobov, Comput. Phys. Comms. 163 (2004) 85.
[27] B.C. Silva, P. Barletta, J.J. Munro, J. Tennyson, J. Chem. Phys. 128 (2008) 244312.
[28] U.V. Riss, H.D. Meyer, J. Phys. B: At. Mol. Opt. Phys. 26 (1993) 4503.
[29] L. Lodi et al., J. Chem. Phys. 128 (2008) 044304.
[30] M.S. Child, R.T. Lawton, Faraday Discuss 71 (1981) 273.
[31] P.D. Chowdary, M. Gruebele, Phys. Rev. Lett. 101 (2008) 250603.